VOLTAGE PROFILE ENHANCEMENT IN A DWINDLING ELECTRIC POWER SYSTEM

J. N Onah, B.O Anyaka , V.C Ukwueze, U.C Ogbuefi.

Abstract— N-1 secure was carried out in a 27-bus of 330kV transmission grid to investigate the low/high voltage violations using Fast Decoupled load flow (FDLF) method owing to its time per numerical iteration in MATLAB environment. It was assumed that voltages less than 0.95pu and greater than 1.05pu are cases of voltage violation scenarios. In order to improve the voltage profiles and increase the grid robustness, unified power flow controller was injected into the buses with voltage violations and the simulation results show improvements in the voltage profile of the network.

Index Terms— contingency analysis, FACTS, Fast decoupled load flow, Load flow, power system stability, Unified power flow controller,voltage profile.

1. INTRODUCTION

The electric power generation-transmission-distribution in developing countries constitutes a large system that exhibits a range of dynamic phenomena [1]. Stabilities of these systems need to be maintained even when subjected to low probability disturbances so that the electricity can be supplied to consumers with high reliability. In the recent time, power demand has increased substantially while the expansion of power generation and transmission has been severely limited. Various controllers such as High voltage dc transmission, static var compensator, have been developed over time to control the dynamic characteristics of power systems. Many of the controllers are on-off switches (circuit breakers) that can isolate short-circuited or malfunctioning equipment, or shed load or generation. Others are discrete controllers like tap changers in transformers or switching of capacitor/reactor banks [1].Still others are continuous Control like voltage controllers and power system stabilizers in rotating generators or the newer

Power electronic controls in FACTS devices (Flexible AC Transmission Systems refers to modern electronic devices like High Voltage DC Transmission or Static VAR Controllers that can control power flows or voltage). However, these controllers are local that is, their input and their control variables are in the same local substation. Most dynamic phenomena in the power system, on the other hand, are regional or sometimes system-wide.

2. POWER SYSTEM STABILITY

Successful operation of a power system depends largely on the engineer's ability to provide reliable and uninterrupted service to the loads. The reliability of the power supply implies much more than merely being available. Ideally, the loads must be fed at constant voltage and frequency at all times. The first requirement of reliable service is to keep the synchronous generators running in parallel and with adequate capacity to meet the load demand. Synchronous machines do not easily fall out of step under normal conditions. A second requirement of reliable electrical service is to maintain the integrity of the power network. The high-voltage transmission system connects the generating stations and the load centers. Power-system stability is a term applied to alternating-current electric power systems, denoting a condition in which the various synchronous machines of the system remain in synchronism, or "in step," with each other. Conversely, instability denotes a condition involving loss of synchronism, or falling "out of step [2]. Djilani [3] identified the placement of the Unified Power Flow Controller (UPFC)

in order to minimize active power losses and improve the voltage profiles with the use of injection model of the (UPFC) in Newton-Raphson load flow algorithm. But the time per iteration of the method is

relatively slow when compared with Fast decoupled load flow method. And Kahyaei [4] investigated the effect of location of IPFC on voltage profile and real and reactive power flow in transmission lines in power system. Naresh et al [5] used Newton-Raphson (NR) power flow algorithm to study the power flow in the power systems network. They further applied interline power flow controller to enhance the voltage profile. An optimal placement strategy based on single line contingencies through performance index was proposed by Suresh [6]. The thyristor switches control the on and off periods of the fixed capacitor and reactor banks and thereby realize a variable reactive impedance. Except for losses, they cannot exchange real power with the system. [7]. A unified power flow controller (UPFC) is the most promising device in the FACTS concept. It has the ability to adjust the three control parameters, *i.e.* the bus voltage, transmission line reactance, and phase angle between two buses, either simultaneously or independently. It combines the excellent features of STATCOM and static synchronous series compensator SSSC [8]. A UPFC performs this through the control of the in-phase voltage, quadrature [7].The placement of UPFC in a transmission line maintains voltage profile and loss minimization due to reactive current as espoused in [9]. In addition, the optimal placement of the device in a transmission line can decongest a loaded line as can be found in [10].

3 LINE LOADABILITY

Line Loadability can be defined as Transmission-line voltages decrease when heavily loaded and increase when lightly loaded. When voltages on EHV lines are maintained within ±5% of rated voltage, corresponding to about 10% voltage regulation, unusual operating problems are not encountered. Ten percent voltage regulation for lower voltage lines including transformer voltage drops is also considered good operating practice.

The load ability of short transmission lines (less than 80 km in length) is usually **determined** by the conductor thermal limit or by ratings of line terminal equipment such as circuit breakers.

For longer line lengths (up to 300 km), line loadability is often determined by the voltage-drop limit. Although more severe voltage drops may be tolerated in some cases, a heavily loaded line with VR/VS ≥ 0.95 is usually considered safe operating practice. For line lengths over 300km, steady-state stability becomes a limiting factor [11]. Line loadability is also used to describe the load carrying ability of a transmission line operating under a specified set of operating condition. In practice transmission lines are not operated to deliver their theoretical maximum power, which is based on rated terminal voltages and an angular displacement, $\delta = 90^0$ across lines. Inductors and capacitors are used on medium length and long transmission lines to increase line load ability and to maintain voltage near rated values. Shunt reactors (inductors) are commonly installed at selected points along EHV lines from each phase to neutral as illustrated in Fig. 2.10. The inductors absorb reactive power and reduce over voltages during light load conditions. They also reduce transient over voltages due to switching and lightning surge. In addition, shunt reactors can reduce line loadability if they are not removed under full load conditions. Shunt capacitors are sometimes used to deliver reactive power and increase transmission voltages during heavy load conditions [12]. Series capacitors are sometimes used on long lines to increase the loadability as shown in figures 1(a) and 1(b). Capacitor banks are installed in series with each phase conductor at selected points along a line. Their effects is to reduce the net series impedance of the line in series with the capacitor bank, thereby reducing line voltage drops and increasing the steady-state stability limit [12].

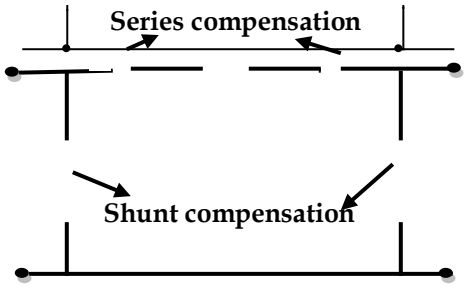

1.(a) Schematic

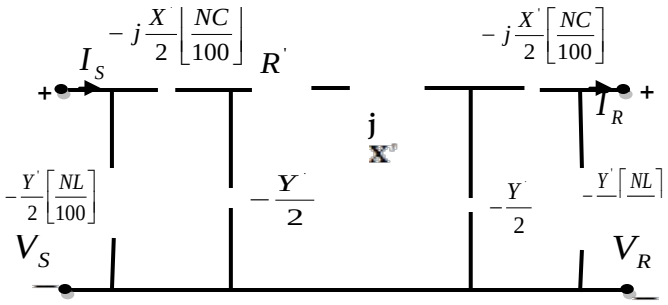

1.(b) Equivalent circuit

Fig.1 Compensated Transmission Line Section

Note NC is the amount of series capacitive compensation; NL is the amount of shunt reactive compensation.

The one line diagram of Nigerian 330kV transmission grid, the generator data, the load data and the line data are respectively shown in figure 2. Table1, table 2 and table 3.

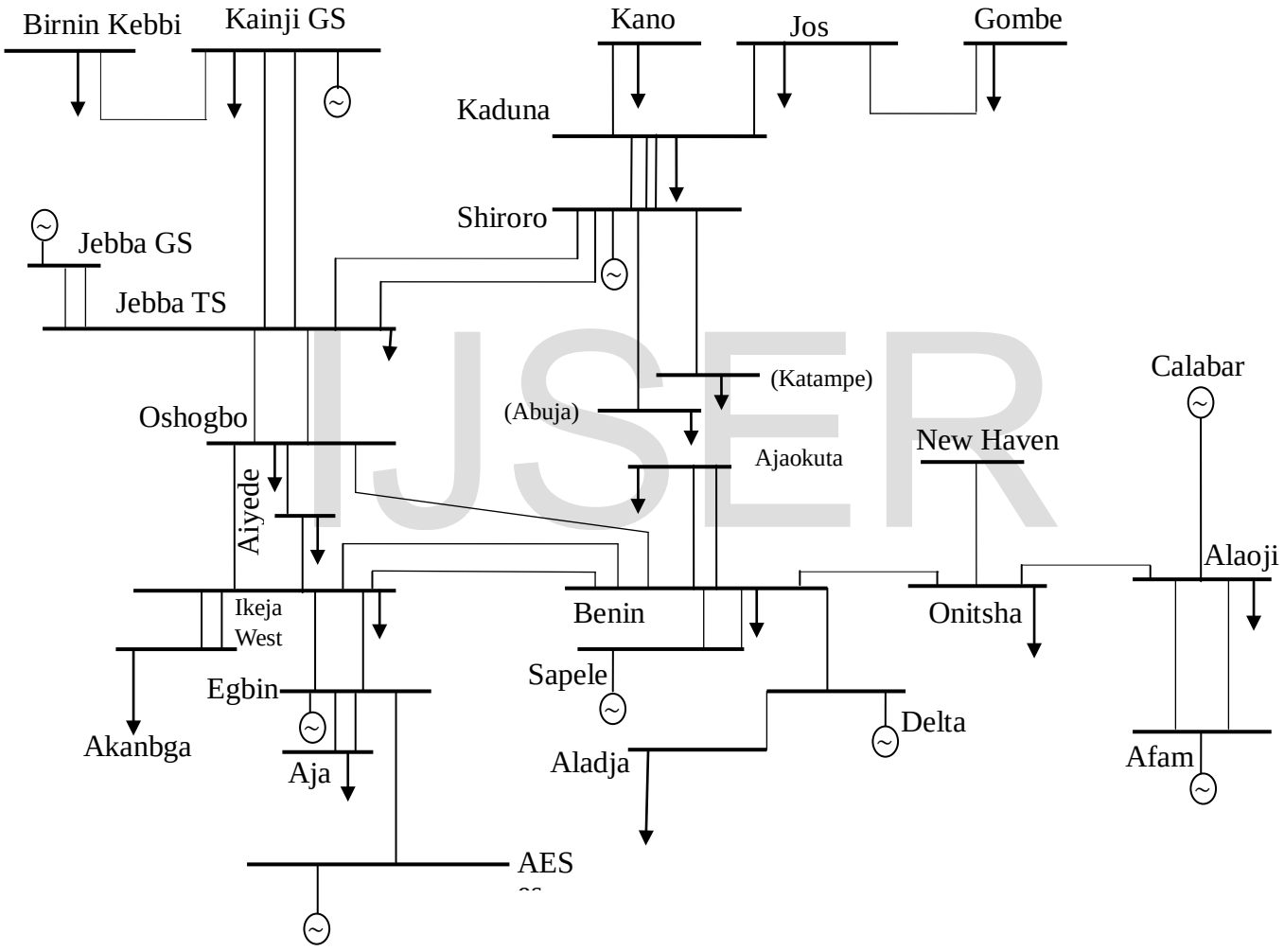

Figure 2 : One line diagram of Nigerian 330kv transmission grid [11].

Table1: Generator Data

S/No.	Bus name	PG(MW) Rated
1	Kainji GS	756
2	Shiroro	413
3	Jebba GS	339
4	Sapele	70
5	Egbin	967
6	Afam	316
7	Delta GS	498
8	AES	235
9	Calabar	0

Source: [11]

Table 2: Load Data

S/No	**Bus Name**	**Active Power (MW)**	**Reactive Power (MVAR)**
10	Birin-kebbi	89	55
11	Kano	226	140
12	Jos	114	90
13	Gombe	130	80
14	Kaduna	260	161
15	Jebba TS	7.44	3.79
16	Katampe	236	146
17	Oshogbo	194	120
18	Ajaokua	72	45
19	New Haven	182	112
20	Aiyede	210	130
21	Ikeja-west	484	300
22	Benin	136	84
23	Onitsha	146	77
24	Alaoji	248	153
25	Akangba	389	241
26	Aja	200	124
27	Aladja	47.997	24.589

Source: [11]

Table 3: Line Data

Branch No.	From	To	R(pu)	X(pu)	B(PU)
1	10	1	0.02676	0.06576	1.178
2	8	5	0.00300	0.02100	0.300
3	9	24	0.00216	0.00530	0.2570
4	1	15	0.00699	0.01718	0.308
5	3	15	0.00069	0.0017	0.033
6	15	17	0.01355	0.0333	0.597
7	17	21	0.02167	0.05324	0.521
8	17	20	0.00993	0.02439	0.437
9	20	21	0.01183	0.02906	0.521
10	21	25	0.00147	0.0361	0.065
11	21	5	0.00535	0.01315	0.257
12	5	26	0.00138	0.00339	0.257
13	21	22	0.02417	0.05939	1.162
14	22	4	0.00432	0.01061	0.208
15	4	27	0.00544	0.01336	0.239
16	7	27	0.00276	0.00679	0.239
17	7	22	0.00924	0.0227	0.239
18	18	22	0.0145	0.03564	0.208
19	17	22	0.02167	0.05324	0.954
20	2	15	0.02106	0.05176	0.927
21	2	16	0.01243	0.03055	0.308
22	14	2	0.00829	0.02036	0.364
23	11	14	0.01985	0.04879	0.874
24	12	14	0.01692	0.04158	0.927
25	12	13	0.002279	0.056	1.01
26	22	23	0.01183	0.02906	0.521
27	19	23	0.00829	0.02036	0.365
28	23	24	0.01191	0.02927	0.524
29	24	6	0.00216	0.0053	0.104

Source: [11]

4. MATHEMATICAL MODEL OF UNIFIED POWER FLOW CONTROLLER [UPFC]

The complex power

$S_L = P_L + jQ_L = I^* V_L$ (1)

$Q_L = \frac{(V_L^* - V_R^*)}{-jX_L} V_L$ (2)

Since $V_R = V_L - \frac{\sigma}{2}$ (3)

$\hat{V}_L = \hat{V}_S + \hat{V}_C$ (4)

$= V\frac{<\sigma}{2} + V_C <^{\beta}$ (5)

P_L and Q_L Can be expressed as

$P_L = P_O + \frac{VV_C}{X_L}\sin\left(\frac{\delta}{2} + \beta\right)$ (6)

$Q_L = Q_O + \frac{VV_c}{X_L} - \frac{VV_C}{X_L}\cos\left(\frac{\delta}{2} + \beta\right) + 2\frac{VV_C}{X_L}\cos\left(\frac{\delta}{2} - \beta\right)$ (7)

Since

$P_{O=}\frac{V^2}{X_L}, \bar{Q}_O = \frac{V^2}{X_L}(1-\cos\delta)$ (8)

Defining

$Q'_O = Q_O + \frac{V^2}{X_L}$ (9)

$(P_L - P_O)^2 (5 - 4\cos\delta) + \left(Q_L - Q'_O\right)^2 - 4(P_L - P_O)\left(Q_L - Q'_O\right)\sin\delta = \frac{V^2 V_C^2}{X_L}(2\cos\delta - 1)^2$ (10)

Substituting equation 6 and equation 7 into equation 1

We have

$S_L = P_O + \frac{VV_C}{X_L}\sin\left(\frac{\delta}{2} + \beta\right)$ (11)

In the above equations, three variables Vs

PL and QL can be regulated by controlling V_C and β. By so doing the disturbance in the system is fixed using Unified power flow controller.

5. MATHEMATICAL MODEL OF TWO-BUS SYSTEM TRANSMISSION LINE OF THE NIGERIAN 330KV TRANSMISSION GRID

The performance of transmission line equation is presented in the form of voltage and current relationship between the sending- and receiving-ends. Since loads are more often expressed in terms of real and reactive powers then, from the single line diagram of a two bus transmission line shown in Fig.4

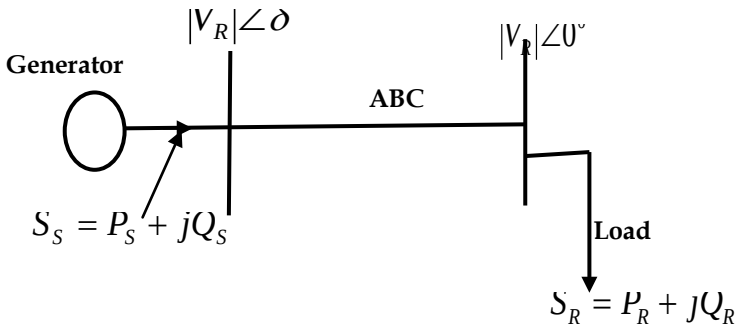

Fig 3: A Two-Bus System of Transmission Line

Taking the receiving-end voltage as a reference phasor i.e. $(V_R = |V_R|\angle 0^0)$ and the sending end voltage $(V_S = |V_S|\angle\delta)$ which leads by an angle δ. The angle δ is torque angle or load angle. It mainly determines the power delivered by the generator and the magnitude of E_f (i.e. excitation voltage) determines the VARs delivered by it.

Complex power leaving the sending-end and entering the receiving-end of the transmission line is expressed (in per phase) as;

$$S_S = P_S + jQ_S = V_S I^*_S \quad (12)$$

Receiving- and sending-end current expressed in terms of receiving- and sending-end voltage can be written as:

$$I_R = \frac{1}{B}V_S - \frac{A}{B}V_R \quad (13)$$

If A, B, D constants are written as

$$A = |A|\angle\alpha, B = |B|\angle\beta, D = |D|\angle\alpha,$$

(Since A =D)

Then the equation (12) and equation (13) can be re-written in the following way.

$$I_R = \left|\frac{1}{B}\right||V_S|\angle(\delta - \beta) - \left|\frac{A}{B}\right||V_R|\angle(\alpha - \beta) \quad (14)$$

$$I_S = \left|\frac{D}{B}\right||V_S|\angle(\alpha + \delta - \beta) - \left|\frac{1}{B}\right||V_R|\angle(-\beta) \quad (15)$$

Substituting in Eq.12 we have

$$S_R = |V_R|\angle 0\left[\left|\frac{1}{B}\right||V_S|\angle(\beta-\delta)-\left|\frac{A}{B}\right||V_R|\angle(\beta-\alpha)\right]$$

$$=\frac{|V_S||V_R|}{|B|}\angle(\beta-\alpha)-\left|\frac{A}{B}\right||V_R|^2\angle(\beta-\alpha) \quad (16)$$

Similarly $S_S = \left|\frac{D}{B}\right||V_S|^2\angle(\beta-\alpha)-\frac{|V_S||V_R|}{|B|}\angle(\beta+\alpha)$

(17)

S_R and S_S are per phase complex volt-amperes (in per phase volts). If V_R and V_S are expressed in KV, then the three-phase receiving-end complex power is given by

$$S_E(3-phaseVA)=3\left\{\frac{|V_S||V_R|\times 10^6}{\sqrt{3}\times\sqrt{3}|B|}\angle(\beta-\delta)-\left|\frac{A}{B}\right|\frac{|V_R|^2}{3}\times 10^6\angle(\beta-\alpha)\right\}$$

$$S_E(3-phaseMVA)=\frac{|V_S||V_R|\angle(\beta-\delta)}{B}-\left|\frac{A}{B}\right||V_R|^2(\beta-\alpha) \quad (19)$$

Eq.16 is same as Eq.17 and the same result holds for S_i. If we express Eq.16 in real and imaginary part we have for real and reactive powers at the receiving –end as:

$$P_R = \frac{|V_S||V_R|}{|B|}\cos(\beta-\delta)-\left|\frac{A}{B}\right||V_R|^2\cos(\beta-\alpha) \quad (20)$$

$$Q_R = \frac{|V_S||V_R|}{|B|}\sin(\beta-\delta)-\left|\frac{A}{B}\right||V_R|^2\sin(\beta-\alpha) \quad (21)$$

Similarly, for real and reactive power at sending-end we have:

$$P_S = \left|\frac{D}{B}\right||V_S|^2\cos(\beta-\alpha)-\frac{|V_S||V_R|}{|B|}\cos(\beta-\delta) \quad (22)$$

$$Q_S = \left|\frac{D}{B}\right||V_S|^2\sin(\beta-\alpha)-\frac{|V_S||V_R|}{|B|}\sin(\beta-\delta) \quad (23)$$

From Eq.19 we can see that the receiving power P_R will be maximum at $\delta=\beta$ that is,

$$P_{R(\max)} = \frac{|V_S||V_R|}{|B|}-\frac{|A||V_R|^2}{B}\cos(\beta-\alpha) \quad (24)$$

And corresponding Q_R is,

$$Q_{R(\max)} = -\frac{|A||V_R|^2}{B}\sin(\beta-\alpha) \quad (25)$$

This means that the load must draw much leading MVAR in order to receive the maximum real power. If we consider a case where we have a short line with a series impedance Z, that is, $A = D = 1\angle 0; B = Z = |Z|\angle 0$

Substituting these in Eqs. 16 and 22 we get the simplified results for the short line as;

$$P_R = \frac{|V_S||V_R|}{|Z|}\cos(\theta-\delta)-\frac{|V_R|^2}{|Z|}\cos\theta \quad (26)$$

And

$$Q_R = \frac{|V_S||V_R|}{|Z|}\sin(\theta-\delta)-\frac{|V_R|^2}{|Z|}\sin\theta \quad (27)$$

Considering the receiving-end and the sending-end;

$$P_S = \frac{|V_S|^2}{|Z|}\cos\theta-\frac{|V_S||V_R|}{|Z|}\cos(\theta+\delta) \quad (28)$$

The above short line equation will also apply for a long line when the line is replaced by its equivalent - $\prod$ or nominal- $\prod$ and the shunt admittances are lumped with the receiving-end load and sending-end generation.

From Eq. 24 the maximum receiving-end power is received when $\delta=\theta$

$$P_{R(\max)} = \frac{|V_S||V_R|}{|Z|}-\frac{|V_R|^2}{|Z|}\cos\theta \quad (29)$$

We replace $\cos\theta$ with $R/|Z|$ that is,

$$P_{R(\max)} = \frac{|V_S||V_R|}{|Z|}-\frac{|V_R|^2}{|Z|^2}R \quad (30)$$

Usually the resistance of a transmission line is small compared to its reactance (since it is necessary to maintain a high efficiency). So that,

$$\theta = \tan^{-1}\frac{X}{R} = 90^0$$

Where, $Z = R + jX$, eqs. 24 and 27 can be approximated as

$$P_R = \frac{|V_S||V_R|}{X}\sin\delta \quad (31)$$

$$Q_R = \frac{|V_S||V_R|}{X}\cos\delta - \frac{|V_R|^2}{X} \qquad (32)$$

For a very long line in the network, voltage cannot be raised beyond the limits placed by present day high voltage technology. To increase power transmitted in such cases, the only choice is to reduce the line reactance. This can be accomplished by the implementation of unified power flow controller (UPFC). The flow chart for the voltage profile improvement, the table for voltage before and after the simulation of UPFC at the outage of Shiroro GS , the histogram showing voltage before and after the simulation of UPFC at the outage of Shiroro GS are respectively shown in figure 4, table 4, and figure 5. The algorithm taken to achieve the desired result is given in the flow chart shown in figure 4

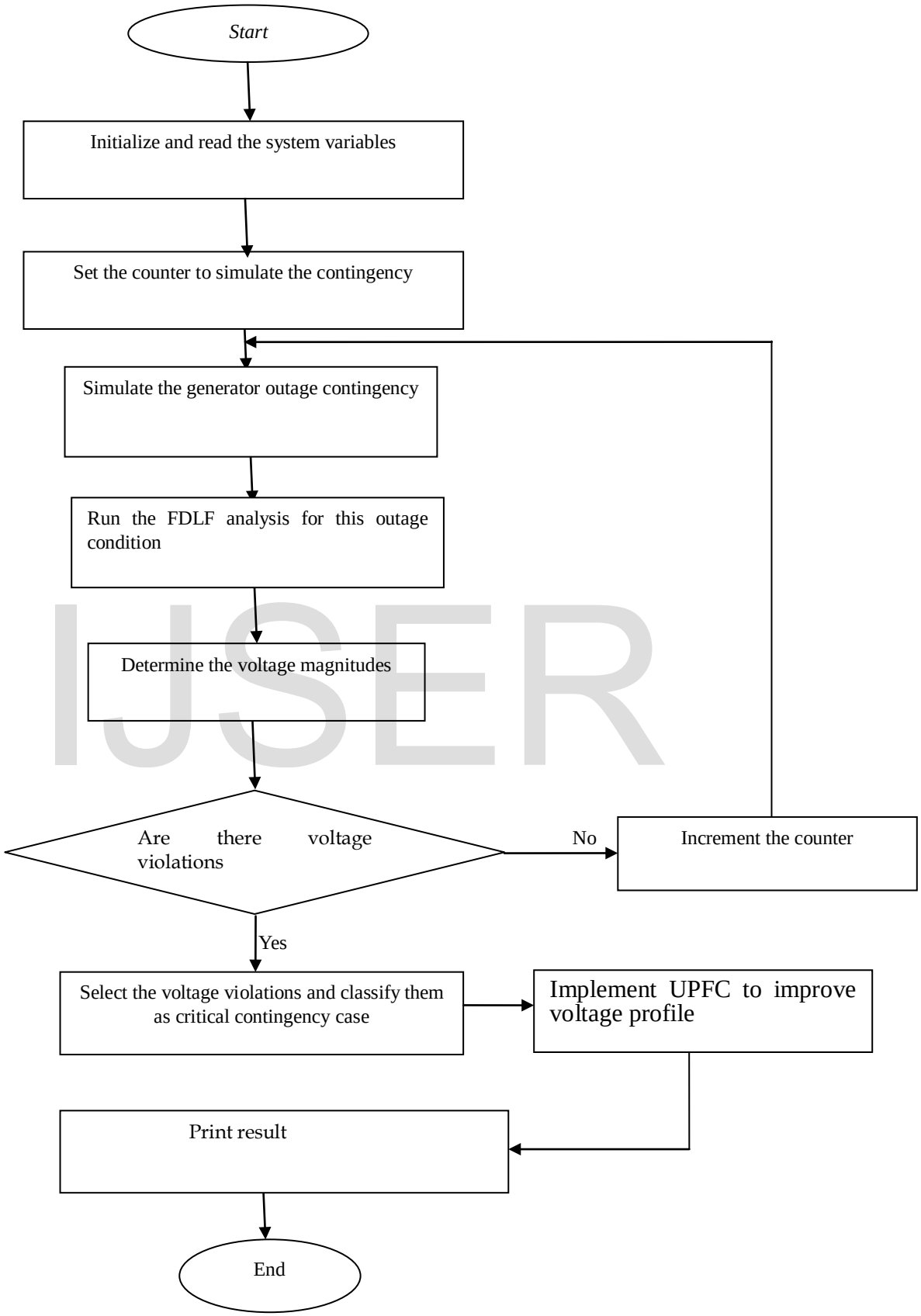
Start
Initialize and read the system variables
Set the counter to simulate the contingency
Simulate the generator outage contingency
Run the FDLF analysis for this outage condition
Determine the voltage magnitudes
Are there voltage violations
No
Increment the counter
Yes
Select the voltage violations and classify them as critical contingency case
Implement UPFC to improve voltage profile
Print result
End

6. SIMULATION OF THE GENERATOR OUTAGE

With various assumptions made in the FDLF the RHS of the equations 33 and (43) contains network admittances that do not change during successive iteration for power flow problems because they are constants. Hence they are evaluated and inverted once, then used in successive iteration. It is due to the nature of the jacobian matrices and the sparsity of their matrices that the solution is fast. The iteration continued until the mismatch in the real power and reactive power are within a specified tolerance. The simulation equations take the form

$$\frac{[\Delta P_i]}{V_i} = [B_i^{'}] \ [\Delta\delta] \qquad (33)$$

$$\frac{[\Delta P_i]}{V_i} = [B_k^{''}] \ [\Delta\delta] \qquad (34)$$

7. RESULTS AND DISCUSSION

The simulation shows that the following buses have low voltage violations as shown in tabe 4 and figure 5. We have Kano, Gombe, Kaduna, Katampe, Oshogbo, Ajaokuta, New Haven, Aiyede, Ikeja-West, Onitsha and Akangba falling below 0.95pu. Then the low voltage violations were boosted up with the aid of UPFC.

Table 4: Voltage before and after the simulation of UPFC at the outage of Shiroro GS

Bus No.	Voltage	
	Mag(pu)	Mag(pu)
1	1.003	1.003
2	1.000	1.000
3	1.000	1.000
4	1.000	1.000
5	1.000	1.000
6	1.000	1.000
7	1.000	1.000
8	1.000	1.000
9	1.000	1.000
10	0.974	0.974
11	0.778	0.988
12	0.751	0.998
13	0.643	0.979
14	0.849	0.996
15	0.993	0.994
16	0.932	0.962
17	0.911	0.984
18	0.943	0.974
19	0.901	0.982
20	0.865	0.989
21	0.878	0.985
22	0.968	0.968
23	0.938	0.964
24	0.990	0.990
25	0.861	0.977
26	0.993	0.993
27	1.000	1.000

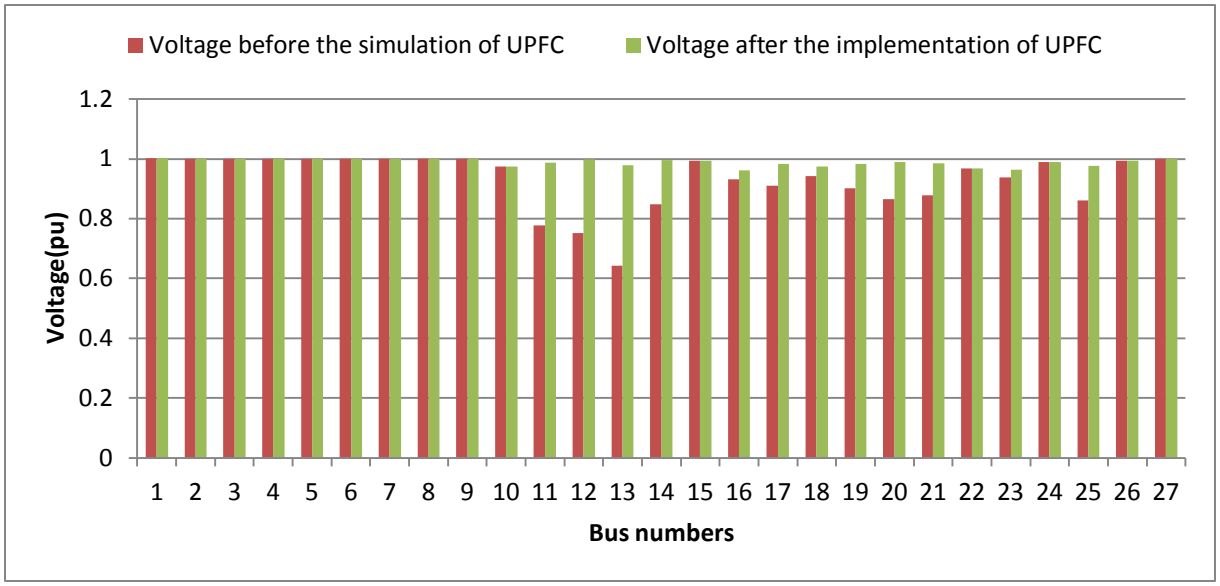

Figure 5: Histogram showing Voltage before and after the simulation of UPFC at the outage of Shiroro GS

8. SUMMARY

Considering the number of numerical iteration per time taken, Fast Decoupled load flow method has proven to be excellent in the load flow analysis of the Nigerian 330kV transmission grid. The load flow studies identified buses with low voltages. At the outage of Shiroro generator bus, it was observed that Kano, Gombe, Kaduna, Katampe, Oshogbo, Ajaokuta, New Haven, Aiyede, Ikeja-West, Onitsha and Akangba were falling below 0.95pu. The UPFC having advantages over other FACTS devices in terms of dynamic response, stability improvement, increase in power transfer capability, power flow control etc was chosen among other FACTS devices for the voltage profile improvement.

REFERENCES

[1] Y. N. Yu, *Electric Power System Dynamics*. New York: Academic Press, 1983.

[2] P. W. Sauer and M. A. Pai, *Power System Dynamics and Stability*. New York: Prentice Hall, 1998

[3] I. Y. Djilani Kobibi, S. Hadjeri, and M. A. Djehaf. "Study of UPFC Optimal Location Considering Loss Reduction and Improvement of Voltage Stability and Power Flow" Leonardo Journal of Sciences.Issue. 24, pp85-100, 2014.

[4] A. Kahyaei. "Analysis of Interline Power Flow Controller (IPFC) Location in Power Transmission Systems" Research Journal of Applied Sciences, Engineering and Technology Issue. 3 Volume.7: pp633-639, 2011.

[5] A. V. Naresh Babu, S. Sivanagaraju, C. Padmanabharaju and T. Ramana. "Power flow analysis of a power system in the presence of interline power flow controller (IPFC)" ARPN Journal of Engineering and Applied Sciences. Volume 5, No. 10, 2010.

[6] C. V. Suresh and S. S Raju. "Mathematical modeling and analysis of a Generalized Unified Power Flow Controller with Device rating Methodology". International Journal on Electrical Engineering and Informatics Volume 7, Number 1, 2015.

[7] IEEE Power Engineering Society, *FACTS Overview*. IEEE Special Publication 95TP108, 1995.

[8] N.G. Hingorani and L. Gyugyi, "Understanding FACTS: concepts and technology of flexible ac transmission systems", IEEE Press, NY, 1999.

[9] A.Farhangfar, S.J. Sajjadi, S. Afsharnia, "Power flow control and loss minimization with Unified Power Flow Controller (UPFC)", IEEE Conference on Electrical and Computer Engineering, 2004, pg: 386– 387 Vol.1.

[10] M. Noroozian, L. Angquist, M. Ghandhari, and G. Andersson, "Use of UPFC for optimal power flow control",

[11] B.O. Anyaka, T. C. Madueme, C. J. Nnonyelu "Power System Contingency Analysis: A Study of Nigeria's 330KV Transmission grid", Proceedings of the Fourth Electrical Engineering National Conference, July 2013.

[12] U. C. Ogbuefi, "Power flow Analysis of Nigerian Power System with compensation on some buses". Unpublished Ph.D Thesis. Department of Electrical Engineering University of Nigeria Nsukka, pp. 15-16. 2013

[13] D. P. Kothari and J. Nagrath. "Mordern Power System Analysis". Third Edition Tata McGraw-Hill publishing Company Ltd. New Delhi, pp. 520, 2003.